Short-range order in the quasiliquid phases of alkane substructures within aperiodic urea inclusion crystals

A. Simonov,[1,2,*] P. Rabiller,[1,†] C. Mariette,[1,‡] L. Guérin,[1] A. Bosak,[3] A. Popov,[3] and B. Toudic[1]

[1]*Institut de Physique de Rennes, UMR UR1-CNRS 6251, Université de Rennes 1, 35042 Rennes, France*

[2]*Department of Materials, ETH Zurich, Vladimir-Prelog-Weg 1-5/10, 8093 Zürich, Switzerland*

[3]*European Synchrotron Radiation Source, 6 rue Horowitz, 38000 Grenoble, France*

(Received 1 December 2021; accepted 25 April 2022; published 15 August 2022)

n-alkane/urea inclusion compounds are prototypical examples of aperiodic crystals with uniformly aligned alkane guest molecules contained within linear channels formed by the supramolecular urea host. Here, we investigate single-crystal diffuse scattering, which is present in the form of sharp layers, from short-chain guest molecules (from octane to dodecane). The strong modulation of diffuse scattering within these layers shows that the positions of alkane molecules in neighboring channels are correlated. Using the three-dimensional difference pair distribution function method, we have extracted the effective interaction potentials and have shown that the interaction is mediated by the relaxation of urea molecules.

DOI: 10.1103/PhysRevB.106.054206

I. INTRODUCTION

Aperiodicity in materials generates very specific properties. From the structural point of view, the translational symmetry, which is lost in the physical space, is recovered in higher-dimensional spaces called crystallographic superspaces [1,2]. From the dynamical point of view, supplementary degrees of freedom are predicted, such as phasons, which are thermal fluctuations along the supplementary (internal) dimensions of the crystallographic superspace [3,4]. Three families of aperiodic crystals can be distinguished: Quasicrystals, incommensurately modulated crystals, and aperiodic composites [4]. The latter family is defined by two or more interpenetrating sublattices with lattice parameters whose ratio is an irrational number along at least one direction.

n-alkane/urea crystals are a prototype family of aperiodic composites. In these crystals, urea molecules connected by hydrogen bonds form a honeycomblike host structure with hexagonal channels that stretch along the c direction and are characterized by the periodicity c_h (Fig. 1). By construction, the channels are filled with linear alkane molecules, which have their own incommensurate periodicity c_g. Much work has been dedicated to various aspects of this system, including collective and individual dynamics and phase transitions [5–26]. For almost all the long-chain, linear alkane guest molecules having the formula n-C_nH_{2n+2}, with $n > 12$, a four-dimensional superspace group describes the whole set of Bragg peaks at room temperature. Since the host and guest share the unit cell axes a and b, the use of four indices $(hklm)$ permits the description of the whole set of diffraction Bragg peaks within the reciprocal space:

$$G_{hklm} = ha^* + kb^* + lc_h^* + mc_g^*.$$

Alkane molecules with <13 carbons do not exhibit long-range order at room temperature. This is evident from the absence of Bragg reflections associated with the guest structure. Instead, the diffraction patterns contain sharp diffuse layers, commonly referred to as s layers [Fig. 1(b)]. The thickness of the layers along c^* is proportional to m^2, which is a sign of the so-called *quasiliquid* or *paracrystalline* incommensurate ordering of alkane molecules within the channels [27–29]. The presence of the urea host structure significantly limits the degrees of freedom available to the guest molecules. This makes diffuse scattering significantly more structured and simplifies its interpretation, as compared with real liquids. Similar phases exist for $HgAsF_6$ and organic salts [28,30–34].

In this paper, we have collected diffuse scattering from urea inclusion compounds with short linear alkanes from *n*-octane to *n*-dodecane at the ESRF synchrotron (*n*-undecane/urea was not considered for reasons given below). Within the s layers, reconstructions showed strong modulation of intensity corresponding to significant interactions between alkanes in neighboring channels. We used the three-dimensional difference pair distribution function (3D-ΔPDF) method [24,35–38] to extract the effective interaction parameters directly from diffuse scattering without explicitly building a disordered incommensurate model. The distribution of alkane molecules in urea/alkane along the host sublattice channels can be interpreted in terms of intrinsic characteristic lengths of both sublattices.

II. EXPERIMENT

The experiments were performed on the *n*-alkane/urea inclusions compounds at room temperature. The single crystals were grown by slowly cooling a solution of the *n*-alkane and urea in *ad hoc* solvents. The diffraction measurements were performed at $\lambda = 0.77$ Å on beamline ID-23 at the ESRF synchrotron, which is equipped with a Pilatus 6M detector.

*arkadiy.simonov@mat.ethz.ch

†philippe.rabiller@univ-rennes1.fr

‡celine.mariette@esrf.fr

Each measurement consisted of a single 360° ω scan with a 0.1° oscillation range per frame.

The crystal orientations were determined with the program XDS [36,39], and the hexagonal unit cell parameters of the host structure were found to be equivalent to the literature values of $a = b = 8.23$ Å, $c_h = 11.02$ Å, with the space group $P6_122$ [8,9,26]. The values of c_g were found to be very close to the relationship reported by Lenné *et al.* [6], being here $c_g(n) = [1.270(n-1) + 3.658]$ Å. Total scattering was reconstructed in reciprocal coordinates using the program MEERKAT [39]. Diffuse scattering consisted of the sharp s layers perpendicular to the c^* direction, thermal diffuse scattering (TDS) around Bragg peaks, as well as broad d bands, which have been previously assigned to the intramolecular carbon-carbon correlations within alkane molecules [8,11,40,41]. Only the main $hk0m$ s planes were used in the refinements.

The s layers of diffuse scattering, at positions mc_g^*, were extracted and integrated along c^*. Layers until $m = \pm 3$ were extracted for n-octane and n-decane, while for n-nonane and n-dodecane, layers were extracted until $m = \pm 4$. The background for each layer was estimated as the average of intensities slightly above and below the layer and was then subtracted. In certain places, where diffuse layers were close to Bragg peaks, the background was overestimated; in such cases, after corrections, negative intensities were observed. These negative intensities were set to zero but nevertheless were included in the calculations to ensure the stability of the refinement. The adjusted layer intensities were averaged over $6/mmm$ Laue symmetry using the outlier rejection procedure of Blessing [42,43] . Of the five crystals, n-undecane/urea was not pursued any further because the proximity of Bragg peaks to the third s-layer line at $(3\gamma \sim l = 2)$ seriously complicated the extraction of reliable diffuse scattering data. Refinement of the diffuse scattering was performed with the program YELL [36] using unit weights. Diffuse scattering extracted in $(hk01)$ and $(hk02)$ layers are reported on Fig. 2 (left part of figure for each compound/layer).

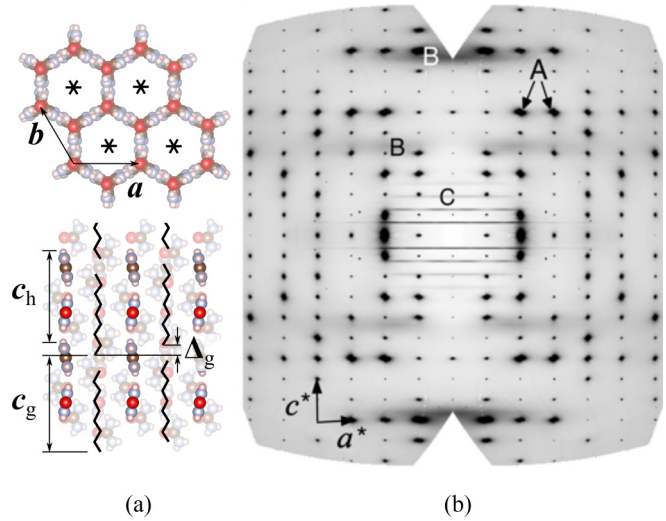

(a) (b)

FIG. 1. (a) The crystal structure of urea inclusion compound. (b) The reconstructed $(h0lm)$ plane of the n-dodecane/urea inclusion compound; diffuse scattering consists of thermal diffuse scattering around Bragg peaks (A), broad diffuse bands (d bands) (B), and sharp $(hk0m)$ s-layers at positions mc_g^* with $c_g^*/c_h^* = \gamma \cong 0.63$ (C).

III. QUALITATIVE 3D-ΔPDF ANALYSIS

The 3D-ΔPDF maps were calculated with the Fourier transform of the intensities extracted from the diffuse scattering layers. Here, 3D-ΔPDF represents the difference between the PDF of the crystal and its Patterson function and can therefore be both positive and negative [36,37]. 3D-ΔPDF maps are analogous to Patterson maps and can be similarly interpreted: Each signal at a position $[u,\ v,\ w]$ corresponds to all of the interatomic *pairs* for which the interatomic vector satisfies the condition $x_2 - x_1 = u$, $y_2 - y_1 = v$, and $z_2 - z_1 = w$, where x, y, and z are expressed in crystallographic fractional coordinates. The 3D-ΔPDF map directly shows the short-range correlations between those pairs: The positive signals (brown) mean that corresponding pairs appear more frequently in the real structure than the average structure; the negative signals (blue) mean the opposite.

The 3D-ΔPDF map for n-dodecane/urea is presented in Fig. 3. The signals can be separated into three regions (see insert on Fig. 3). The first (marked 1 in the figure) corresponds to the center of the channel and shows positive and negative signals that repeat periodically along the channel axis. This means that, within a channel, alkane molecules are arranged almost periodically, in full agreement with the paracrystalline model [19]. The correlations near the lattice points marked 3 show a similar positive-negative alternation along c, albeit with lower intensities. These signals correspond to the correlations in positions between alkanes in neighboring channels. In the $uv0$ section, the flowerlike shape around the central feature (marked 2) corresponds to interatomic vectors between the alkanes and urea. This characteristic shape is caused by the relaxation of the urea walls around the alkane molecules (the so-called size effect) [35].

Due to the limited number of observed layers, the resolution along c is very coarse, corresponding to 1.7–2.5 Å for different alkanes; thus, individual interatomic vectors could not be resolved. Instead, only the overall shape of the molecule is visible. This is illustrated in Fig. 4, which shows the 3D-ΔPDF map that would have been observed in an ideal experiment in which (i) TDS is not present, (ii) all of the s planes and d bands can be measured out to 0.5 Å resolution, and (iii) all of the alkane molecules are in the all-anti conformation and in the same orientation. In such a case, individual interatomic vectors within a molecule are clearly visible as sharp positive peaks. Due to the paracrystalline behavior, the correlations between different molecules become progressively weaker as the distance increases.

Note the presence of negative (blue) signals around positions $w = \pm c_g/2$, $\pm 3c_g/2$, etc. These signals arise because the calculation of 3D-ΔPDF does not include the Bragg peaks that this paracrystalline phase exhibits in the $hk0$ plane. These peaks are shared by the host and the guest substructures and thus cannot be easily used for analyzing the guest behavior. Omission of these peaks lowers the PDF signals by subtracting a constant value, in such a way that the projection of the 3D-ΔPDF signal onto the uv plane equals zero.

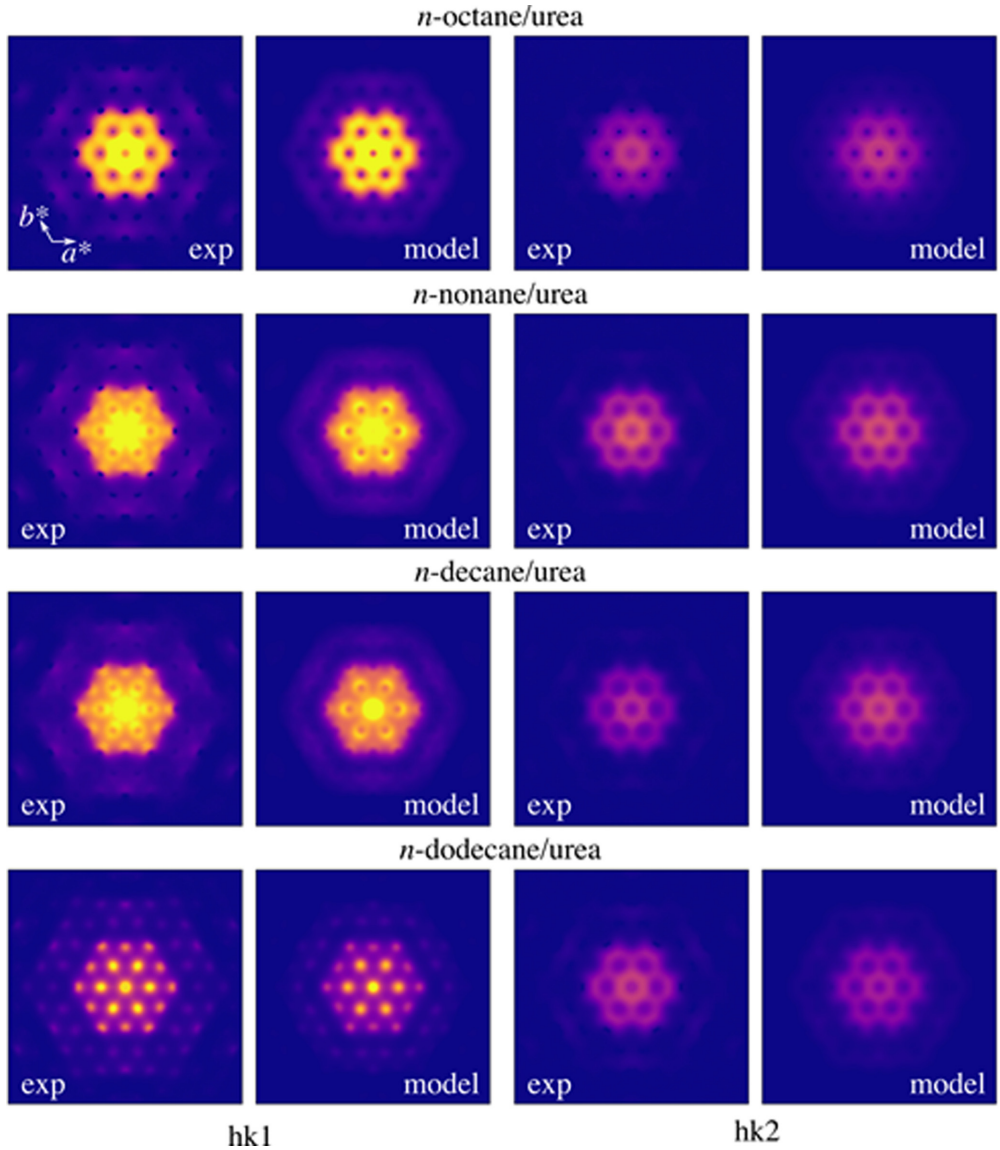

FIG. 2. Calculated and modeled diffuse scattering from the (hk01) (left) and (hk02) (right) s layers of the crystals in this paper. The diffuse scattering is presented in a shape of hexagons or clouds centered at the position of Bragg peaks. Reciprocal unit cell is essentially identical for all the crystals and is drawn for the hk1 layer of n-alkane compound.

In the real 3D-ΔPDF process, the profiles of s planes were not measured along the c axis at a single position but were instead integrated along the c^* direction over their full width. This integration effectively convolves all intramolecular and intermolecular correlations [Fig. 4(c)]. The integration procedure also gives the resulting 3D-ΔPDF map a periodicity of c_g along the c axis. Furthermore, as already noted, in the real experiment, the intensities of s planes decay very quickly. Thus, depending on the alkane length, only three or four planes can be measured reliably. This dramatically reduces the resolution of the 3D-ΔPDF maps [Fig. 4(d)].

The calculated 3D-ΔPDF maps were fit in the program YELL, which allows one to find the optimal model parameters with least-squares minimization against the experimental data. Such refinements are performed in PDF space and do not require one to explicitly construct an atomic model. Currently, YELL works in 3D space and does not support a higher dimensional crystallographic formalism, which is required for a full description of this system, including host Bragg peaks and guest diffuse scattering planes. However, a 3D description was sufficient to model the sharp diffuse planes, which are associated with the guest substructure. In an analogous fashion, the average structure of these compounds is fully described by the 3D $P6_122$ symmetry of the host.

The 3D-ΔPDF model comprises three parts, as shown in the following subsections.

A. Alkane molecules within the channels

It was assumed that the alkanes adopt all-anti conformations. This was modeled by forming a zigzag chain between atoms with a C-C distance of 1.54 Å and a corresponding distance along the channel axis of 1.27 Å. The displacement in the (a, b) plane was along the ($2y$, y, 0) direction (toward the

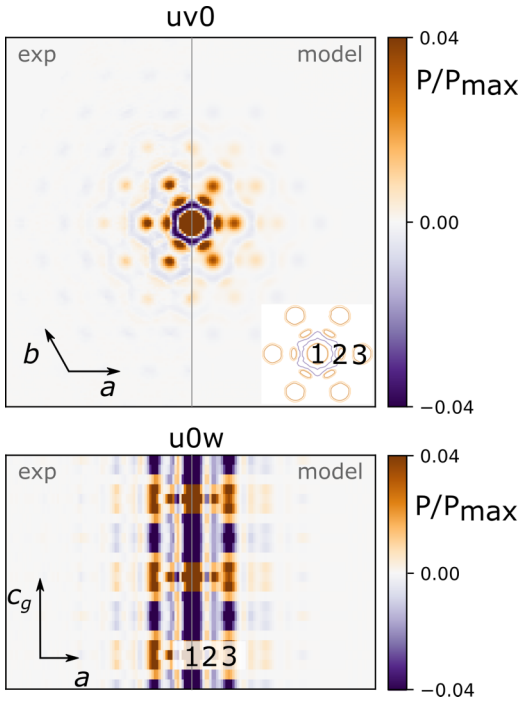

FIG. 3. Comparison between experiment and model 3D-ΔPDF map for *n*-dodecane/urea inclusion compound, sections $uv0$ and $u0w$. The strongest contrast represents the correlation between alkane molecules within the same channel (1), relaxation of urea walls around the alkanes (2), and correlation between alkane molecules in the neighboring channels (3).

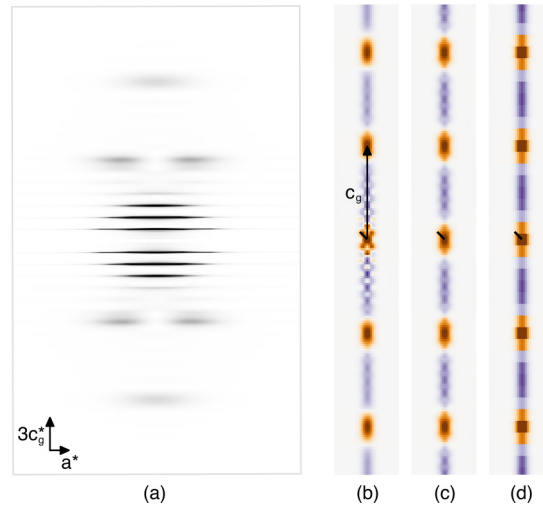

FIG. 4. (a) Diffuse scattering in the (a^*, c^*) plane, and (b) 3D-ΔPDF map for an idealized paracrystalline phase of *n*-dodecane molecules in urea channels. (c) The 3D-ΔPDF map after integration of diffuse scattering features using a window corresponding to the reciprocal length of the alkane. (d) The 3D-ΔPDF map obtained from the first four s layers. The diagonal black lines show the distances between adjacent carbons within the *n*-alkane molecules.

corner of the hexagons). Due to rotational averaging, displacement of the atoms toward the sides of the hexagon would have given an identical refinement. Each atom was assigned atomic displacement parameters $U_{11} = U_{22} = 0.3\,\text{Å}^2$, $U_{33} = 0.1\,\text{Å}^2$, which were found empirically to provide the correct decay of the model diffuse scattering with the scattering vector. The molecules were rotationally disordered, and it was assumed that all six equivalent orientations of the molecules are present with equal probabilities to give overall $p6/mmm$ rod group symmetry.

In contrast to Welberry and Mayo [16], our model contained no correlations between molecular orientations. The conclusions of Welberry and Mayo [16] are based on diffuse scattering in the ($hk00$) plane, whereas in this paper we account for s-diffuse scattering in ($hk0m$) layers, which is absent in the ($hk00$) plane. Also note that diffuse scattering in the ($hk00$) allows for different interpretation. In two papers, we interpreted it in terms of dynamic TDS around strong Bragg peaks and pretransitional diffuse scattering around the critical wave vectors associated with the phase transitions [44,45].

As the guest molecules arrange in a paracrystalline manner, the long-range order vanishes along the channel directions. It is observed experimentally a characteristic broadening of s layers which follows the law $w(m) = m^2(\pi\,\Delta_m/c_g)^2$, where $w(m)$ is the half-width half maximum of the s layers which have Lorentzian profiles along c^* [27,28,46,47]. The dependence of the parameter Δ_m vs alkane length is reported later in the discussion (see Fig. 8 in Sec. IV). In 3D-ΔPDF, the paracrystalline model consisted of N intermolecular pairs. For each pair, the joint displacement parameter U_{zz} of a molecule, as seen from another molecule, was set to $U_{zz} = g\Delta r_z$, where Δr_z is the distance between the molecules along the channel axis, and g defines how well the molecular positions are correlated [48]. It was found that three neighbors are sufficient to describe the chain.

B. Nearest neighbor interactions

As discussed in the introduction, the *n*-alkane/urea family is a prototypical example of aperiodic composite crystals in which the misfit parameter γ is ordinarily not a rational number, so the crystal is translationally disordered, and alkane molecules in neighboring channels can occupy a range of relative positions along the channel axis (Δ_g). In our model, the relative positions of guests in adjacent channels were approximated with discrete set of positions. We defined as many positions as allowed by the (limited) resolution of diffuse scattering data along c^*. For *n*-octane and *n*-decane, there were six fractional positions: 0, $\frac{1}{6}$, $\frac{2}{6}$, … $\frac{5}{6}$; for *n*-nonane and *n*-dodecane, there were eight positions: 0, $\frac{1}{8}$, $\frac{2}{8}$, … $\frac{7}{8}$. The resulting steps were large, ∼1.7–2.5 Å for different alkanes.

As noted above, the positions of alkane molecules in neighboring channels are not independent. 3D-ΔPDF allows us to refine the probability $p(\Delta_g)$ of relative displacement of alkane molecules in the neighboring channels Δ_g [see Fig. 1(a)] and thus provides insight into the free energies (G) associated with such displacements:

$$G(\Delta_g) = -\ln[p(\Delta_g)] + C.$$

The probabilities were restricted by symmetry. As an approximation, we assumed rotationally averaged molecular

$p6/mmm$ symmetry, to give

$$p\left(\frac{i}{N_{\text{pix}}}\right) = p\left(\frac{N_{\text{pix}} - i}{N_{\text{pix}}}\right),$$

where N_{pix} is the number of pixels along the c axis. In addition to the constraint on probabilities summing up to unity, this led to one independent parameter per neighbor per measured diffuse scattering layer. The correlations for the first five lateral neighbors [1, 0], [2, 0], [2, 1], [3, 0], and [3, 1] were refined; however, in all compounds, significant correlations were observed only for the nearest neighbors.

C. Wall corrugation

The 3D-ΔPDF maps show that urea walls relax around the alkane molecules. Modeling the urea molecules in this case is subtle because, as already noted, urea periodicity is incommensurate with that of alkane molecules. Here, we use the same technique used for modeling the alkane, when refining the average host structure [9]: When seen from the point of view of the alkane substructure, the urea walls appear as electron density which is continuous in the c direction. The interaction between alkane and urea molecules is manifested as a modulation of the urea in the (a, b) plane depending on $\Delta z'$, the relative position of urea with respect to alkane molecules [49].

IV. RESULTS AND DISCUSSION

The models were refined in the program YELL to give R values of 12.7, 14.0, 19.3, and 17% for n-octane, n-nonane, n-decane, and n-dodecane, respectively. The modeled diffuse scattering (Fig. 2) and the 3D-ΔPDF match very well with the experimental results. The latter is presented in Fig. 3 for n-dodecane/urea. The relative energies of interactions between alkanes in neighboring channels are presented in Fig. 5.

The alkane-alkane interactions are most likely mediated by the relaxation of urea molecules, which were found to be very similar in all investigated crystals. As an example, the relaxation of n-dodecane/urea crystal is presented in Fig. 6. Oxygen atoms show almost no displacement, while the carbon and nitrogen atoms move away from alkane and toward the van der Waals gap between guest molecules within a channel, with an amplitude of ∼0.3 Å. Torsion dynamics, including end groups and gauche defaults which are mainly located at the ends of alkane molecules, as found by Le Lann *et al.* [18,50], but also probably nonlinear modes [51], are most likely correlated with urea displacements, and this may be a key feature of the various behaviors observed in alkane urea inclusion compounds.

The relative energy distribution is periodic and even; thus, Fourier analysis can be performed using only cosine terms, and due to sampling conditions, it can be performed up to order 4 for n-decane and n-octane and up to order 3 for n-dodecane and n-nonane. As can be seen in Fig. 5, second-order fit is not enough, except for n-decane, and order 4 only improves for n-nonane. From obtained relative energies, probability densities can be computed. For an ideal infinite incommensurate composite, the displacement shift Δ_g/c_h should be uniformly distributed in the [0, 1] interval. The

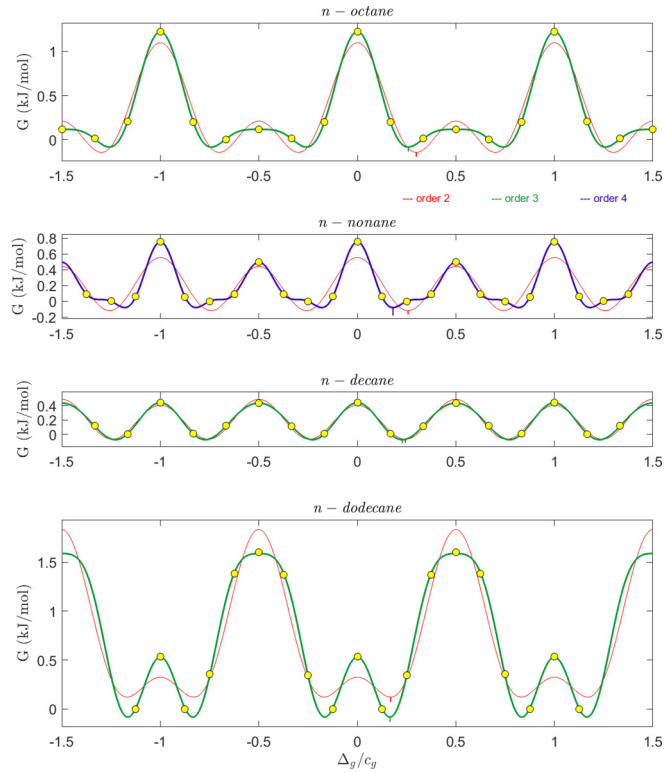

FIG. 5. The free energy of interaction between alkane molecules in neighboring channels as a function of displacement of guests in neighboring channels (Δ_g/c_h). Values shown by circles were obtained from YELL, whereas the lines are fits of Fourier coefficients up to order 3 (n-dodecane, n-nonane) or up to order 4 (n-decane, n-octane). The color coding of solid lines corresponds to the fit order: Red ($n = 2$), green ($n = 3$), and dark blue ($n = 4$).

computed probability densities $\rho(\Delta_g/c_g)$, plotted in Fig. 7, are normalized to the equipartition. The amplitude of the relative deviation from equipartition ranges up to ∼20% and is smaller for n-decane and n-nonane.

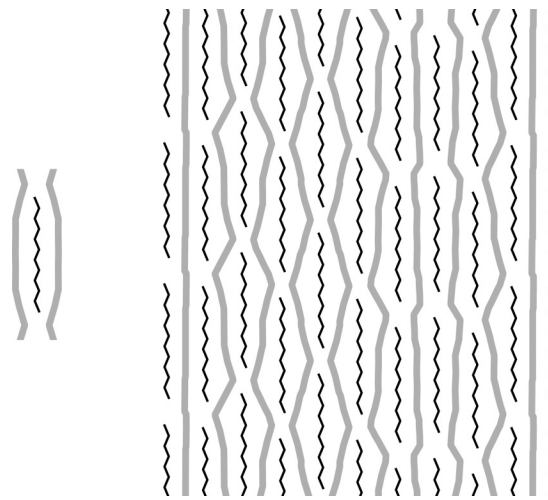

FIG. 6. The relaxation of urea walls (gray) in an n-dodecane/urea structure; the dynamic disorder of alkane molecules is not shown.

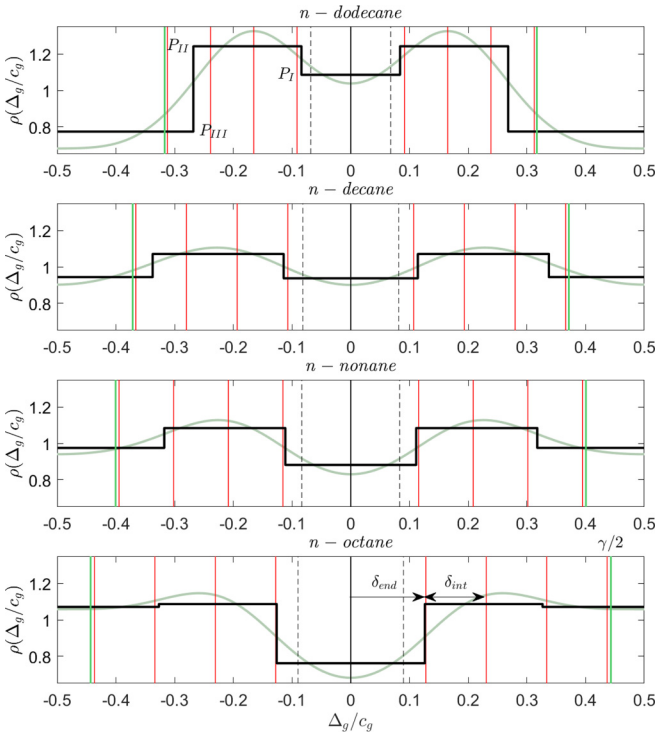

FIG. 7. Density probabilities normalized to equipartition for *n*-octane, *n*-nonane, *n*-dodecane, and *n*-decane, as a function of the relative shift Δ_g/c_g between alkane molecules from channel to channel. Solid smooth gray curves are computed from relative energy Fourier decomposition. Black crenel functions correspond to an extrapolated simplified model used for analysis in terms of internal characteristic lengths. Vertical markers correspond to (light blue) half the host periodicity $\gamma/2$, (dashed black) the standard deviation of the shift, and (dotted red lines) shift steps corresponding to "end groups" (δ_{end}) and internal periodicity (δ_{int}) of sixfold averaged alkane molecules (i.e., 1.27 Å).

As Fourier decomposition is limited to order 3 or 4, a schematic crenel function model is drawn (see Fig. 7), revealing three regions of interest in the probability distribution. The first region (I) is centered on zero shift, corresponding to the minimum of probability, except for *n*-dodecane where it is a local minimum above equipartition value. Two side regions are observed, a first one (II) corresponding to the maximum of probability and an another one (III) corresponding to a local minimum of probability on approaching the $\frac{1}{2}$ molecule shift. Although corresponding to the average value, the zero shift is not favored. A minimum shift $\delta_{\text{end}} \approx 1.6 \pm 0.1$ Å is found, and then the most probable shifts extend over a distance corresponding to ∼3 times the internal periodicity of sixfold averaged alkane molecules (i.e., $\delta_{\text{int}} \approx 1.27$ Å). One can notice that the distance corresponding to four internal periods matches with half of the host periodicity, i.e., the periodicity, located at $\gamma/2$ in reduced coordinates, seen by sixfold averaged alkane chains due to the double urea helix of host sublattice induced by the $P6_122$ symmetry. The minimum shift δ_{end} and further extent over few alkane internal periods δ_{int} can be associated with the observed relaxation of urea molecules previously described, which may be accommodated by the van der Waals gaps between adjacent

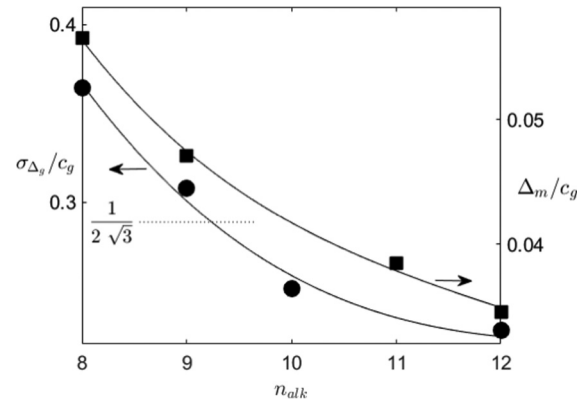

FIG. 8. (Left axis) Standard deviation of the relative shift between alkane chains from channel to channel, and (right axis) characteristic parameter of disorder of the second kind along the alkane channels.

alkane molecules within a channel or by torsional modes of the alkane molecules. When two gaps are aligned, urea molecules are not displaced toward either gap. If the two gaps are displaced by a few angstroms, the urea can rotate toward both gaps at the same time, and the mobile alkane end groups can explore the additional volumes of space provided, assisted by the dynamic of torsional modes which mainly take place near the end groups. For larger displacements, e.g., when the gap between two alkanes is laterally aligned with the center of an alkane in an adjacent channel, the urea can move toward the gap; at the same time, however, the less flexible central portion of the alkane on the other side of the channel wall cannot move out of the way of the turned urea. The latter effect is more significant for longer alkanes, which explains why the observed energy penalty for $\Delta_g = c_g/2$ is the largest in the *n*-dodecane/urea system.

The probability distribution being periodic and even, the average shift between alkane molecules is zero, and the standard deviation departs <20% from the $1/(2\sqrt{3})$ value corresponding to uniform equipartition. The standard deviation monotonically increases with decreasing the alkane length (Fig. 8). It correlates with the observed characteristic parameter Δ_m of the second kind of disorder of alkane chains [46,52] and is consistent with the increased instability found for short alkane urea inclusion compounds.

V. CONCLUSIONS

The problem of short-range order in quasiliquid phases is a very complicated one. Here, we have taken advantage of several properties of a prototype family of aperiodic host/guest organic composites to tackle this question. First, aperiodicity allows an infinite number of equivalent relative positions of the guest confined subsystem within the host [1]. This is at the origin of the zero or nearly zero energy sliding mode along this aperiodic direction [3]. Secondly, in the case of *n*-alkane/urea compounds, the host structure forms parallel channels that confine the linear alkane molecules and thus provides nice examples of one-dimensional subsystems. The paracrystalline nature of this subsystem was demonstrated

earlier [19]. High-resolution synchrotron x-ray measurements performed on single crystals containing guests with chain lengths ranging from 8 to 12 reveal a rich intensity modulation within the different scattering planes associated with these paracrystalline guest phases. Diffuse scattering was analyzed using the 3D-ΔPDF method. It is shown that the diffuse layers from these single crystals of urea inclusion compounds can be described by a model assuming (a) within the channels, the alkane molecules are arranged periodically to form a paracrystal, (b) the position of alkanes in the nearest channels are correlated, and the correlation decreases quickly with distance, (c) the urea framework relaxes by pushing away from the alkane and into the gap between alkane molecules, and (d) the analysis of probability distribution of the shift between adjacent alkane molecules argues in favor of such a relaxation mechanism being assisted by the torsional modes occurring close to the ends of alkane molecules. These results constitute an example of direct analysis of short-range order in one-dimensional quasiliquids. Because of extraordinary experimental advances at synchrotron facilities, with respect to both beam flux and detector capabilities, similar 3D-ΔPDF approaches promise to become standard ways of treating complex crystallographic problems in the presence of disorder.

ACKNOWLEDGMENT

The authors thank M. D. Hollingsworth for providing the crystals and for fruitful discussions. A.S. was supported by the Swiss National Science Foundation (Grant No. PZ00P2_180035).

[1] T. Janssen, A. Janner, A. Looijenga-Vos, and P. M. de Wolff, Incommensurate and Commensurate Modulated Structures, in *International Tables for Crystallography Volume C: Mathematical, Physical and Chemical Tables*, edited by E. Prince (Springer Netherlands, Dordrecht, 2004), pp. 907–955.

[2] S. van Smaalen, *Incommensurate Crystallography* (Oxford University Press, Oxford, 2007).

[3] R. Blinc and A. Levanyuk, *Incommensurate Phases in Dielectrics* (North Holland, Amsterdam, 1986),Vol. 14.2.

[4] T. Janssen, G. Chapuis, and M. de Boissieu, *Aperiodic Crystals: From Modulated Phases to Quasicrystals* (Oxford University Press, Oxford, 2007).

[5] A. E. Smith, The crystal structure of the urea-hydrocarbon complexes, Acta Cryst. A **5**, 224 (1952).

[6] H.-U. Lenné, H.-C. Mez, and W. Schlenk, Moleküllängen in Einschlußkanälen von Harnstoff und Thioharnstoff, Liebigs Ann. Chem. **732**, 70 (1970).

[7] Y. Chatani, Y. Taki, and H. Tadokoro, Low-Temperature form of urea adducts with *n*-paraffins, Acta Cryst B **33**, 1 (1977).

[8] R. Forst, H. Jagodzinski, H. Boysen, and F. Frey, Diffuse scattering and disorder in urea inclusion compounds $OC(NH_2)_2 + C_nH_{2n+2}$, Acta Cryst B **43**, 187 (1987).

[9] R. Forst, H. Jagodzinski, H. Boysen, and F. Frey, The disordered crystal structure of urea inclusion compounds $OC(NH_2)_2 + CH_{2n+2}$, Acta Cryst B **46**, 70 (1990).

[10] K. Fukao, Disorder in paraffin chains of urea adducts and *n*-paraffins, J. Chem. Phys. **92**, 6867 (1990).

[11] K. Fukao, T. Horiuchi, S. Taki, and K. Matsushige, Phase transitions of urea adducts with n-paraffins under high pressure, Mol. Cryst. Liq. Cryst. **180**, 405 (1990).

[12] R. M. Lynden-Bell, The orientational order/disorder phase transition of urea-paraffin inclusion compounds, Mol. Phys. **79**, 313 (1993).

[13] M. D. Hollingsworth and K. D. M. Harris, *Comprehensive Supramolecular Chemistry: Solid-State Supramolecular Chemistry: Crystal Engineering*, Vol. 6 (Pergamon, 1996), p. 177.

[14] R. Lefort, J. Etrillard, B. Toudic, F. Guillaume, T. Breczewski, and P. Bourges, Incommensurate Intermodulation of an Organic Intergrowth Compound Observed by Neutron Scattering, Phys. Rev. Lett. **77**, 4027 (1996).

[15] T. Weber, H. Boysen, M. Honal, F. Frey, and R. B. Neder, Diffuse and satellite scattering in urea inclusion compounds with various alkane molecules, Z. Kristallogr. Cryst. Mater. **211**, 238 (1996).

[16] T. Welberry and S. Mayo, Diffuse x-ray scattering and Monte-Carlo study of guest–host interactions in urea inclusion compounds, J. Appl. Cryst. **29**, 353 (1996).

[17] L. Yeo and K. D. M. Harris, Definitive structural characterization of the conventional low-temperature host structure in urea inclusion compounds, Acta Cryst B **53**, 5 (1997).

[18] H. Le Lann, C. Odin, B. Toudic, J. C. Ameline, J. Gallier, F. Guillaume, and T. Breczewski, Single-Crystal deuterium NMR study of the symmetry breaking in an incommensurate organic inclusion compound, Phys. Rev. B **62**, 5442 (2000).

[19] T. Weber, H. Boysen, and F. Frey, Longitudinal positional ordering of n-alkane molecules in urea inclusion compounds, Acta Cryst B **56**, 132 (2000).

[20] B. Toudic, F. Aubert, C. Ecolivet, P. Bourges, and T. Breczewski, Pressure-Induced Lock-In in an Aperiodic Nanoporous Crystal, Phys. Rev. Lett. **96**, 145503 (2006).

[21] B. Toudic, P. Garcia, C. Odin, P. Rabiller, C. Ecolivet, E. Collet, P. Bourges, G. J. McIntyre, M. D. Hollingsworth, and T. Breczewski, Hidden degrees of freedom in aperiodic materials, Science **319**, 69 (2008).

[22] B. Toudic, P. Rabiller, L. Bourgeois, M. Huard, C. Ecolivet, G. J. McIntyre, P. Bourges, T. Breczewski, and T. Janssen, Temperature-pressure phase diagram of an aperiodic host guest compound, EPL **93**, 16003 (2011).

[23] C. Mariette, M. Huard, P. Rabiller, S. M. Nichols, C. Ecolivet, T. Janssen, K. E. Alquist, M. D. Hollingsworth, and B. Toudic, A molecular "phase ordering" phase transition leading to a modulated aperiodic composite in *n*-heptane/urea, J. Chem. Phys. **136**, 104507 (2012).

[24] L. Guérin, C. Mariette, P. Rabiller, M. Huard, S. Ravy, P. Fertey, S. M. Nichols, B. Wang, S. C. B. Mannsfeld, T. Weber *et al.*, Long-range modulation of a composite crystal in a five-dimensional superspace, Phys. Rev. B **91**, 184101 (2015).

[25] S. Zerdane, C. Mariette, G. J. McIntyre, M.-H. Lemée-Cailleau, P. Rabiller, L. Guérin, J. C. Ameline, and B. Toudic, Neutron Laue and x-ray diffraction study of a new crystallographic

superspace phase in *n*-nonadecane-urea, Acta Cryst B **71**, 293 (2015).

[26] J. L. Atwood and F. Toda, *Comprehensive Supramolecular Chemistry: Solid-State Supramolecular Chemistry: Crystal Engineering*, Vol. 6 (Pergamon, 1996), p. 465.

[27] A. Guinier, *X-Ray Diffraction in Crystals, Imperfect Crystals, and Amorphous Bodies* (Dover Courier Corporation, 1994), Chap. 9, p. 295.

[28] R. Spal, C.-E. Chen, T. Egami, P. J. Nigrey, and A. J. Heeger, X-ray scattering study of one-dimensional lattice dynamics in $Hg_{3-\delta}AsF_6$, Phys. Rev. B **21**, 3110 (1980).

[29] P. M. Chaikin and T. C. Lubensky, *Principles of Condensed Matter Physics* (Cambridge University Press, Cambridge, 1995).

[30] J. M. Hastings, J. P. Pouget, G. Shirane, A. J. Heeger, N. D. Miro, and A. G. MacDiarmid, One-Dimensional Phonons and "Phase-Ordering" Phase Transition in $Hg_{3-\delta}AsF_6$, Phys. Rev. Lett. **39**, 1484 (1977).

[31] I. U. Heilmann, J. D. Axe, J. M. Hastings, G. Shirane, A. J. Heeger, and A. G. MacDiarmid, Neutron investigation of the dynamical properties of the mercury-chain compound $Hg_{3-\delta}AsF_6$, Phys. Rev. B **20**, 751 (1979).

[32] F. Frey and H. Boysen, Low dimensional diffuse scattering, Phase Trans. **67**, 245 (1998).

[33] P. A. Albouy, J. P. Pouget, and H. Strzelecka, X-ray study of the order-disorder phase transition in the triiodide chain compound tetraphenyldithiapyranylidene iodide $[DIPS\Phi_4(I_3)_{0.76}]$, Phys. Rev. B **35**, 173 (1987).

[34] C. Noguera and P. Le Guennec, Quasi-one-dimensional solid-liquid phase transition in compounds containing iodine trimers, Phys. Rev. B **37**, 492 (1988).

[35] T. Weber and A. Simonov, The three-dimensional pair distribution function analysis of disordered single crystals: Basic concepts, Z. Kristallogr. Cryst. Mater. **227**, 238 (2012).

[36] A. Simonov, T. Weber, and W. Steurer, YELL: A computer program for diffuse scattering analysis via three-dimensional delta pair distribution function refinement, J. Appl. Cryst. **47**, 1146 (2014).

[37] R. J. Koch, N. Roth, Y. Liu, O. Ivashko, A.-C. Dippel, C. Petrovic, B. B. Iversen, M. v Zimmermann, and E. S. Bozin, On single-crystal total scattering data reduction and correction protocols for analysis in direct space, Acta Cryst A **77**, 6 (2021).

[38] L. Guérin, T. Yoshida, E. Zatterin, A. Simonov, D. Chernyshov, H. Iguchi, B. Toudic, S. Takaishi, and M. Yamashita, Elucidating 2D charge-density-wave atomic structure in an MX-chain by the 3D-Δpair distribution function method, ChemPhysChem **23**, e202100857 (2022).

[39] A. Simonov, MEERKAT, https://github.com/aglie/meerkat (2015).

[40] K. Fukao, X-ray scattering and disordered structure of *n*-tetracosane in urea adducts. I. A model for the x-ray scattering pattern, J. Chem. Phys. **101**, 7882 (1994).

[41] B. Toudic, H. Le Lann, F. Guillaume, R. E. Lechner, J. Ollivier, and P. Bourges, Coherent neutron scattering analysis of alkane dynamical disorder inside nanoporous urea intergrowth crystals, Chem. Phys. **292**, 191 (2003).

[42] R. H. Blessing, Outlier treatment in data merging, J. Appl. Crystallogr. **30**, 421 (1997).

[43] The pixel i was considered to be an outlier if $|I_i - I_{\text{median}}| > 3\,\underset{k}{\text{median}}(|I_k - I_{\text{median}}|)$, where I_i and I_k are the intensities of the pixels i and k correspondingly, $I_{\text{median}} = \underset{k}{\text{median}}(I_k)$, and the median is taken over all symmetry equivalents. (For details, see Blessing [42], Eqs. (16) and (17) with $c_1 = c_2 = c_4 = 0$, $c_3 = 3$.)

[44] C. Mariette, L. Guérin, P. Rabiller, C. Ecolivet, P. García-Orduña, P. Bourges, A. Bosak, D. de Sanctis, M. D. Hollingsworth, T. Janssen *et al.*, Critical phenomena in higher dimensional Spaces: The Hexagonal-to-Orthorhombic phase transition in aperiodic *n*-nonadecane/urea, Phys. Rev. B **87**, 104101 (2013).

[45] C. Mariette, L. Guérin, P. Rabiller, C. Odin, M. Verezhak, A. Bosak, P. Bourges, C. Ecolivet, and B. Toudic, High spatial resolution studies of phase transitions within organic aperiodic crystals, Phys. Rev. B **101**, 184107 (2020).

[46] T. Weber, Modulierte Strukturen und Fehlordnung in Harnstoffeinschlussverbindungen bei Temperaturen von 30 bis 300 K, Ph.D. thesis, Ludwig Maximilians-Universität München (1997).

[47] C. Mariette, L. Guérin, P. Rabiller, Y.-S. Chen, A. Bosak, A. Popov, M. D. Hollingsworth, and B. Toudic, The creation of modulated monoclinic aperiodic composites in *n*-alkane/urea compounds, Z. Kristallogr. Cryst. Mater. **230**, 5 (2015).

[48] In this paper, we do not report the refined value of g because, in the refinement, it showed a 99% correlation with the scale coefficient describing the total amount of measured diffuse scattering. A proper determination of g should consider the thickness of the s layers along c^*, as discussed in Refs. [19,46].

[49] See Supplemental Material at http://link.aps.org/supplemental/10.1103/PhysRevB.106.054206 for the 3D-ΔPDF maps and refined models of investigated alkane/urea inclusion compounds.

[50] J. Schmider and K. Müller, 2H NMR investigations of the hexadecane/urea inclusion compound, J. Phys. Chem. A **102**, 1181 (1998).

[51] V. V. Smirnov and L. I. Manevitch, Nonlinear torsion dynamics of the *n*-paraffin crystal, Mater. Phys. Mech. **35**, 167 (2018).

[52] C. Mariette, Brisures de symétrie dans des superespaces cristallographiques: Aspects structuruaux et dynamiques, Ph.D. thesis, Université Rennes 1, 2013.